https://doi.org/10.1016/j.energy.2019.116838

Quantifying uncertainty in the aggregate energy flexibility of high-rise residential building clusters considering stochastic occupancy and occupant behavior

Maomao Hu[a,b], Fu Xiao[a,1]

[a] Department of Building Services Engineering, The Hong Kong Polytechnic University, Kowloon, Hong Kong

[b] Research Institute for Sustainable Urban Development, The Hong Kong Polytechnic University, Kowloon, Hong Kong

Abstract

Modern buildings are expected to be not only energy efficient but also energy flexible to facilitate reliable integration of intermittent renewable energy sources into smart grids. Estimating the aggregate energy-flexibility potential at a cluster level plays a key role in assessing financial benefits and service area for energy-flexibility services at design stage and determining real-time pricings at operating stage. However, most existing studies focused on the energy flexibility of individual buildings rather than building clusters. In addition, due to the intrinsic uncertainty in building envelope parameters, performance of building energy systems, and occupancy and occupant behavior, it is necessary to quantify the uncertainty in aggregate energy flexibility. In this study, we developed an approach to quantifying the uncertainty in the aggregate energy flexibility of residential building clusters using a data-driven stochastic occupancy model that can capture the stochasticity of occupancy patterns. A questionnaire survey was carried out to collect occupancy time-series data in Hong Kong for occupancy model identification. Aggregation analysis was conducted considering various building archetypes and occupancy patterns. The uncertainty in aggregate energy flexibility was then quantified based on the proposed performance indices using Monte Carlo technique. With the scaling up of building clusters, the estimated energy-flexibility potential became steady and the weekly energy flexibility stayed around 12.40%. However, the weekly uncertainty of aggregated energy flexibility exponentially decreased from 19.12% for 8 households to 0.74% for 5,120

[1] Corresponding author. Tel.: +852 2766 4194; Fax: +852 2765 7198
E-mail address: linda.xiao@polyu.edu.hk

households, which means that the estimate of a building cluster's energy flexibility is more reliable than that of a single building.

Keywords: Energy flexibility; Load aggregation; Uncertainty analysis; Stochastic occupant behavior; Building clusters.

Nomenclature

A	area, m^2
A	system matrix in state-space model
AC	air conditioner
B	input matrix in state-space model
C	equivalent overall thermal capacitance, J/K
cap	cooling capacity of the air conditioner
COP	coefficient of performance
CV	coefficient of variance
d	disturbance vector
DEF	deterministic energy flexibility
E	energy consumption during a period
E	disturbance matrix in state-space model
EF	energy flexibility
EIR	energy input ration of the air conditioner
f	conversion coefficients for heat gains
HVAC	heating, ventilation and air conditioning system
I	global solar radiation
k	time step
MCMC	Markov Chain Monte Carlo model
N	normal distribution
n	sampling times
p	transition probability
P	transition probability matrix
Q	heat gains, W
R	equivalent overall thermal resistance, K/W
RC	resistance-capacitance model
RES	renewable energy sources
RMSE	root mean square error
s	occupancy state
S	operating signal of AC
T	temperature, ℃
T	triangular distribution
T	system state vector
t	a specific time
TRN	TRNSYS
u	input vector

U	uniform distribution
UEF	uncertainty of energy flexibility
X	Markov-chain, a time sequence
x	the element in Markov-chain
Greek symbols	
δ	control dead-band
δ	standard deviation
μ	mean value
Subscripts	
db	dry-bulb temperature
ext	external surface of wall
in	indoor air
int	internal surface of wall
inter	internal heat gains
m	internal thermal mass
o	outdoor air
rated	the rated operation condition of the air conditioner
set	set-point
solar	solar radiation
w	wall
win	window

1. Introduction

Renewable energy sources (RESs) have increasingly penetrated electric grids and energy markets in recent years to displace the use of fossil fuels and reduce greenhouse gas emissions. The wide integration of RESs, however, influences the reliability of power systems because RESs are intrinsically intermittent and difficult to forecast [1-3]. The peak power consumption at the demand side under severe hot or cold weather conditions sometimes causes a power imbalance, which also adversely affects the reliability of power systems [4]. Buildings are responsible for around 40% of the total energy consumption worldwide and consume over 90% of the total electricity in Hong Kong [5, 6]. As the major end users of electricity, buildings have significant potential to provide peak power reduction and alleviate the power imbalance. In this context, modern buildings are expected to be not only energy efficient but also energy flexible and grid-responsive [7].

1.1. Energy-flexible buildings and building clusters

As defined in IEA EBC Annex 67, the energy flexibility of a building refers to "*the ability to manage its demand and generation according to local climate conditions,*

user needs, and energy network requirements" [8]. Energy systems in buildings play a significant role in providing energy flexibility because they account for substantial electricity consumption, which can be reduced by using building energy management systems [4].

Over the last few years, many studies have focused on the investigation of energy flexibility of energy systems in individual buildings. Dréau and Heiselberg [9] investigated the flexibility potential of two residential houses with different levels of insulation and air-tightness considering both energy performance and occupants' thermal comfort. The passive house with its higher heating inertia was found to have a larger influence on the control strategies for energy flexibility. Shafie-khah et al. [10] applied hybrid phase-change materials (PCMs) in a residential building to provide demand flexibility. Their results showed that the integration of PCMs affected the indoor thermal dynamics and the electricity cost savings under various demand response programs. Three different thermal energy storage tanks, i.e., water, PCMs, and thermochemical material tanks, were integrated with the heating system in an office building to provide demand flexibility [11]. Some studies have put emphasis on the development of energy-flexibility control strategies for heating, ventilation, and air-conditioning (HVAC) systems in individual buildings. Temperature set-point reset [12, 13] and pre-cooling/heating [14, 15] are two common control strategies for providing load reduction and shifting. Yin and Kara et al. [12] applied a set-point change strategy to cooling systems in both residential and commercial buildings to reduce load during on-peak hours. The hourly power reduction potential of HVAC systems for each type of building was assessed under various thermostat adjustment strategies. Hu and Xiao et al. [13, 14] combined temperature set-point reset and pre-cooling strategies for residential air conditioners to shift the energy consumption from high-price to low-price time periods using a genetic algorithm. An advanced model predictive control method was developed by Hu and Xiao et al. [16] for a floor heating system to provide energy flexibility during on-peak hours. Their model simultaneously considered weather conditions, occupancy, and dynamic electricity prices from electric utilities.

Compared with the studies on individual buildings, fewer studies have focused on energy flexibility at the building cluster/community/neighborhood level. Vigna and Pernetti et al. [17] proposed a new definition of building cluster, identified the concept of an energy-flexible building cluster, and reviewed several candidate indicators for

evaluating energy flexibility at the building cluster level. Taniguchi et al. [18] investigated the peak power reduction potential of 5,000 residential households in Japan using various energy-saving measures. A bottom-up energy performance model was developed to assess energy flexibility that considered household composition, floor area, insulation level, etc. Perfumo and Kofman et al. [19] developed a mathematical model to characterize the aggregate dynamics of thermostatically controlled loads on a large scale (10,000 air conditioners) and proposed a control strategy based on the developed model to conduct demand-side load management. Goy and Finn [20] noted that differences in building thermal characteristics, end-use equipment, and occupant behavior need to be considered when estimating energy-flexibility potential on a large scale.

To sum up, investigating the aggregate energy-flexibility potential of thousands of buildings at the cluster/neighborhood/community scale is more meaningful in practice, because the estimation of such amount of flexibility can help system operators assess whether it is financially worthwhile to provide energy-flexibility services, plan how large the service area needs to be at the design stage, and determine the real-time penalty signals (e.g., prices and CO_2) to end-use customers at the operating stage [17, 21]. However, it is not yet sufficiently addressed, and more research efforts are needed. A big remaining challenge is the quantification of the uncertainty in the aggregate energy consumption and energy flexibility at an area level considering the increasing number of building clusters and various influential uncertainty sources (e.g., building design parameters and occupancy). There was a lack of an effective approach to addressing this challenge in the existing research on energy flexibility.

1.2. Uncertainty analysis in building energy assessment

Assessing building energy performance is uncertain because the variables that influence performance, i.e., weather conditions, the thermal parameters of the building envelope, the parameters and control methods of building energy systems, and occupancy and occupant behavior, are intrinsically uncertain. Uncertainty analysis in building energy assessment therefore has attracted increasing attention in recent years.

A large portion of existing studies on the uncertainty analysis of building energy performance focus on the uncertainty of building envelope parameters [22] and HVAC system configurations [23]. Domínguez-Munoz et al. [24] evaluated the effects of the

uncertainty of building envelopes on building peak cooling load based on a simplified resistance and capacity (RC) thermal model. After the sensitivity analysis, they found that the dominant uncertainties were internal mass and the convective heat transfer coefficient between the internal mass and the air. Huang et al. [25] quantified the uncertainty in building peak load by considering 12 uncertain input parameters, including the physical parameters of the envelope. The uncertainty in peak load was then used to size a HVAC system with the assistance of a multi-criterion decision-making technique. In [23], uncertainty in the performance of chillers, cooling towers, pumps, and fans in HVAC systems was considered in the life-cycle analysis of near-zero energy buildings. Wilde et al. [26] proposed a method to predict uncertainty-based life-cycle building energy performance, which considered property changes due to the deterioration of components, maintenance procedures, etc. Moreover, occupancy and occupant energy-related behavior are also recognized as major sources of uncertainty. These sources represent more than 30% of the discrepancy in building energy performance [27]. Several comprehensive literature reviews on state-of-the-art research of occupancy behavior in buildings have been published in the past three years [28-30]. To capture the stochasticity and diversity of occupant behavior, various stochastic occupancy modeling methods have been developed and applied to building performance simulations, including Markov chains [31, 32], the Bernoulli process [33], and survival analysis [34].

Like building energy consumption, energy flexibility is also uncertain because it is essentially the energy consumption deviation between the baseline case and the energy-flexible case. Although there have been extensive studies on the uncertainty analysis of building energy performance, few studies have focused on the analysis of the uncertainty in aggregate energy consumption and energy flexibility at the cluster/community/neighborhood level. Moreover, considering that occupant energy-related behavior is a major source of uncertainty, stochastic occupancy modeling methods need to be used in the uncertainty analysis of the aggregate energy flexibility of building clusters [22].

1.3. Innovations and contributions

To address the aforementioned problems and challenges, we developed an approach to quantifying the uncertainty in the aggregate energy flexibility of residential building clusters using a data-driven stochastic occupancy model. The major contributions of

this study are: (1) a data-driven stochastic occupancy model was developed and identified using questionnaire survey data to capture the dynamics, stochasticity, and diversity in occupancy patterns in today's Hong Kong residential buildings with typical household sizes and composition types; (2) aggregation analysis was conducted to quantify the aggregate energy flexibility of residential building clusters based on various types of building archetypes and occupancy patterns. For each air-conditioned room, the developed stochastic occupancy model was integrated with the data-driven building thermal model developed in our previous work [13] to predict building energy performance under the baseline case and energy-flexible case, resulting in the energy flexibility potential; and (3) Performance indices are proposed to quantify the uncertainty in energy flexibility at a specific time (e.g., hourly and sub-hourly) and during a particular time period (e.g., daily and weekly). Based on the proposed performance indices, the uncertainty in the aggregate energy flexibility of various scales of building clusters was quantified using the Monte Carlo sampling technique.

The rest of this paper is organized as follows. Section 2 introduces the overview of the proposed uncertainty quantification method for the aggregated energy flexibility of residential building clusters. Section 3 presents the development of the data-driven stochastic occupancy model, building thermal model, and the detailed method for quantifying the uncertainty in the aggregate energy flexibility. The validation and test conditions for the proposed method are presented in Section 4. In Section 5, the performances of the data-driven occupancy model and the building thermal model are first tested. The deterministic and uncertainty-based energy flexibility of building clusters of various scales are then investigated. Finally, conclusions are presented in Section 6.

2. Overview of the proposed uncertainty quantification method

The aggregated energy-flexibility potential of building clusters in a residential community is uncertain due to the stochastic nature of various influential variables, including weather conditions, building envelope parameters, performance of building energy systems, and occupancy and occupant behavior. An approach is proposed in this paper for quantifying the uncertainty in energy flexibility of scaled-up building clusters. As shown in Fig. 1, the developed approach consists of four steps: (1) development of data-driven models, including a stochastic occupancy model trained using questionnaire survey data and a building thermal model trained using TRNSYS data;

(2) energy performance analysis of a single air-conditioned room based on the developed data-driven models; (3) aggregation analysis of the energy performance of building clusters of increasing scale; (4) uncertainty analysis of aggregate energy performance (energy consumption and energy flexibility) of the various building clusters using the Monte Carlo sampling technique.

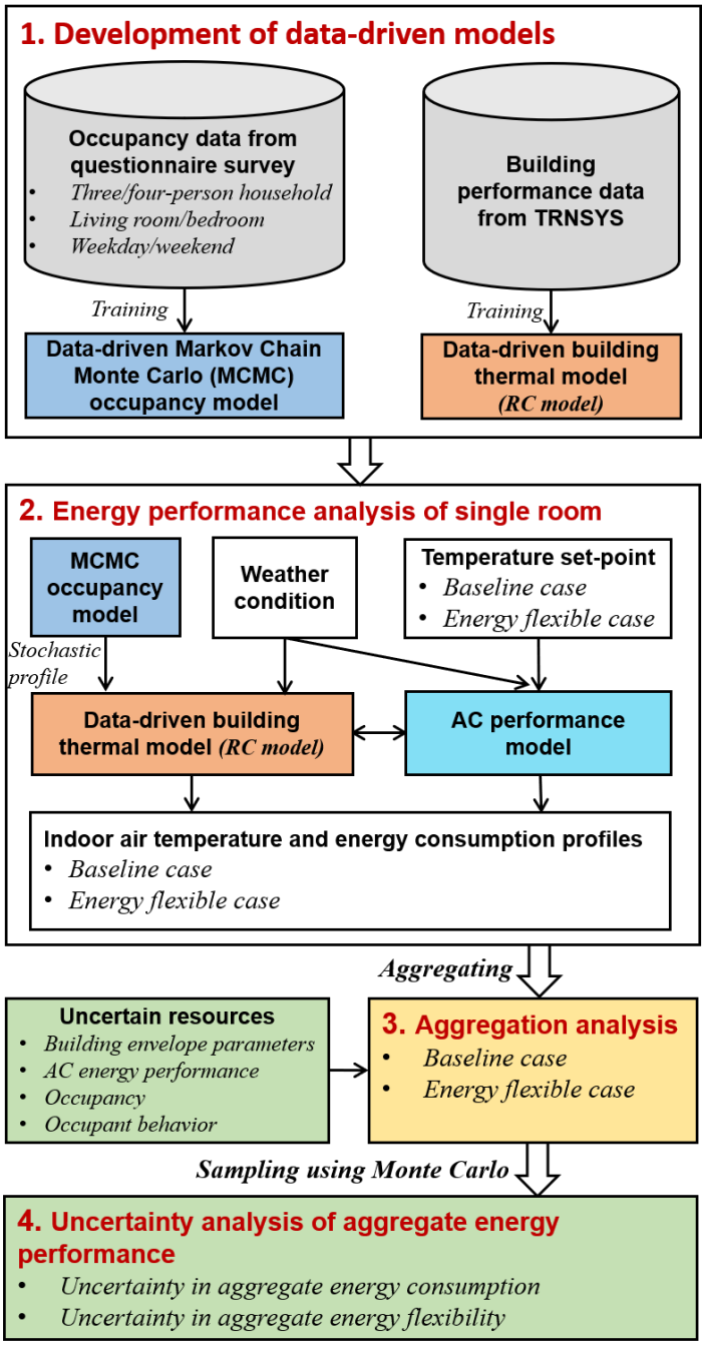

Fig. 1. Flowchart of the proposed approach for quantifying the uncertainty in the aggregate energy flexibility of building clusters.

In Step 1, a Markov-chain Monte Carlo (MCMC) data-driven occupancy model was first developed and then identified using the occupancy time-series data collected by a questionnaire survey. The collected occupancy data were categorized by household size (3-person/4-person), room function (living room/bedroom), and day of the week (weekday/weekend). Considering the computational efficiency for large-scale prediction, a simple data-driven building thermal model (RC model) developed in our previous study [13] was used to predict the building thermal response. Building performance data from either field tests or simulation platforms can be used to identify the parameters in the RC model. In Step 2, An air-conditioner energy performance model was integrated with the building thermal model to predict the dynamic energy consumption of the air-conditioner under changing weather conditions. The developed MCMC occupancy model was used to generate the stochastic occupancy profile as an input of the building thermal model. For comparison, baseline and energy-flexible cases with different indoor air temperature set-points were carried out, resulting in different profiles of indoor air temperature and energy consumption. In Step 3, the energy consumption profiles of all air-conditioned rooms generated in Step 2 were aggregated according to various building archetypes and occupancy patterns to obtain the total energy consumption profile of building clusters in a residential community. In Step 4, the uncertainty in energy consumption and energy flexibility of building clusters was quantified considering the uncertainty sources, including the building envelope parameters, air-conditioner (AC) energy performance, occupancy, and occupancy behavior.

3. Development of models and method for quantifying uncertainty in aggregate energy flexibility

3.1. Data-driven stochastic occupancy modeling

Occupant behavior is a major factor in assessing the uncertainty of building energy performance. Occupancy models are normally developed and integrated with building energy modeling tools to better predict building energy consumption and assess energy management strategies. Occupancy models can be categorized into three basic types based on the occupancy resolution: (1) the occupancy status of a space (occupied/unoccupied), (2) the number of occupants in a space, and (3) the location tracking of an occupant [28, 33]. In this study, the occupancy status information of a space was accurate enough for the energy-flexibility analysis of residential buildings.

3.1.1. A heterogeneous Markov-chain occupancy model

Occupancy can be modeled as a stochastic process, which characterizes the randomness of people entering or leaving a specified space at a particular time. A first-order Markov-chain technique is widely used to simulate that process and to generate stochastic occupancy patterns [32, 35-37].

Here, it is assumed that an air-conditioned space has two states $\{s_0 \quad s_1\}$, representing binary occupancy, i.e., unoccupied and occupied. Define a Markov-chain X as a time sequence $\{x_1 \quad x_2 \quad \cdots \quad x_k\}$, where the Markov chain can take values from the states $\{s_0 \quad s_1\}$ at each time step. The key assumption of a first-order Markov-chain method is that the present state of the occupant is influenced only by the previous state (called a Markovian property). Thus, the probability of state transition from s_i to s_j at time step k, i.e., transition probability $p_{i,j}(k)$, can be given by Eq. (1-a).

$$p_{i,j}(k) = p\left(x_{k+1} = s_j \middle| x_k = s_i\right) \tag{1-a}$$

where $p\left(x_{k+1} = s_j \middle| x_1, x_2, \dots, x_k\right) = p\left(x_{k+1} = s_j \middle| x_k\right)$. When the transition probabilities vary in time, the Markov process is called a heterogeneous Markov chain. The transition probabilities between various states at time step k can be ordered in a transition matrix $\boldsymbol{P}(k)$, as shown in Eq. (1-b). Then, starting from $k = 1$, the probabilities of occupancy states at each time step are given by Eq. (1-c).

$$\boldsymbol{P}(k) = \begin{bmatrix} p_{00}(k) & p_{01}(k) \\ p_{10}(k) & p_{11}(k) \end{bmatrix} \tag{1-b}$$

$$[p_0(k) \quad p_1(k)] = [p_0(1) \quad p_1(1)] \prod_{n=1}^{k-1} \boldsymbol{P}(n) \tag{1-c}$$

where $\sum_{j=0}^{1} p_{ij} = 1$ for each $i \in [0,1]$. Assume that the total number of changes from state i is $n_i(\mathrm{k}) = \sum_{j=0}^{1} n_{ij}(k)$, then the transition probability is estimated by Eq. (1-d).

$$p_{i,j}(k) = \frac{n_{ij}(k)}{n_i(\mathrm{k})} \tag{1-d}$$

The transition probability matrix $\boldsymbol{P}(k)$ at each time step can be derived from the surveyed occupancy data. During the forward occupancy prediction, a uniform distribution is used to generate a random number between 0 and 1. The random number is then compared with the transition probabilities to determine which transition is taking place. This is commonly known as the MCMC technique [31].

3.1.2. Questionnaire survey for occupancy data collection

Occupancy time-series data needed to be collected and processed to identify the transition probability matrices in the Markov-chain model. A questionnaire survey was used in this study to obtain the typical occupancy patterns of the residents of high-rise residential buildings in Hong Kong. A questionnaire survey is effective and reliable, and it reduces occupants' concerns over privacy issues compared with real-time monitoring.

Hong Kong has its own special domestic housing types, household sizes, and household composition types, all of which had an influence on the selection of the occupancy survey samples. The total number of domestic housing units in Hong Kong was 2,534,700 in 2017 [38]. The major housing types are private permanent housing (53.7%), public rental housing (30.5%), and subsidized home ownership housing (14.9%). Compared with the other housing types, public rental housing households have standardized architectural designs because they are planned and constructed by the Housing Department of the Hong Kong SAR government. The average domestic household size is 2.8 persons per household among all housing types and 3.4 persons per household for public rental housing. Regarding the household composition, 64% of households in Hong Kong in 2016 were a nuclear family household, which is defined as a household comprising a couple/a couple with unmarried child(ren)/a lone parent with unmarried child(ren) [39]. In light of the housing and household characteristics in Hong Kong, considering the standardized architectural design of public rental housing, 3-person/4-person public housing households were chosen to represent occupancy patterns in Hong Kong.

Before the distribution of the formal questionnaires, a pre-test survey involving 10 households was carried out to improve the final questionnaire design. The formal questionnaire was divided into two sections. Section A collected basic household information, including housing type, household size, household composition type, floor area, numbers of living/dining rooms and bedrooms, etc. In Section B, the respondents were required to indicate the occupancy status of each room in their flats on an hourly basis for both weekdays and weekends/holidays. The occupancy patterns in summer were requested because air conditioners are normally not operated in winter in Hong Kong. To avoid misunderstandings and ensure the effectiveness of the survey, the

content and objectives of the questionnaire were explained to at least one household member before they started to answer the questionnaire.

3.2. Data-driven building thermal model and AC performance model

3.2.1. Building thermal model

Predicting the energy consumption of AC systems requires a building thermal model that can characterize the building thermal dynamics when subjected to changing influential factors such as weather condition, occupant behavior, and control variable adjustment. Building thermal models can be categorized as white-box, gray-box, or black-box models. White-box models, such as the building thermal models in EnergyPlus and TRNSYS, are labor-intensive and time-consuming. Black-box models are purely data-driven and mainly use statistical tools and machine-learning techniques to analyze large amounts of historical data. Gray-box models, a hybrid of white-box and black-box models, combines basic prior knowledge of building thermal features with a reasonable amount of measured data. They have been proven to be effective and reliable for predicting building thermal responses, with limited need for physical knowledge and training data [40]. RC (resistance and capacity) thermal network gray-box models are widely used to describe space thermal dynamics [41].

A gray-box RC room thermal model was developed, identified, and validated in our previous study [13]. The model can learn the thermal characteristics of the to-be-controlled space by analyzing the data collected from smart in-home sensors. The RC model was developed to capture the thermal dynamics of four major components, i.e., the external wall surface $T_{w,ext}$, internal wall surface $T_{w,int}$, indoor air T_{in}, and internal thermal mass T_m. The energy balances of the components are given by Eqs. (2-a)–(2-d).

$$C_w \frac{dT_{w,ext}}{dt} = \frac{T_o - T_{w,ext}}{R_{w,o}} + \frac{T_{w,int} - T_{w,ext}}{R_w} + Q_{solar,w} \quad (2\text{-a})$$

$$C_w \frac{dT_{w,int}}{dt} = \frac{T_{w,ext} - T_{w,int}}{R_w} + \frac{T_{in} - T_{w,int}}{R_{w,in}} \quad (2\text{-b})$$

$$C_{in} \frac{dT_{in}}{dt} = \frac{T_m - T_{in}}{R_{in,m}} + \frac{T_{w,int} - T_{in}}{R_{w,in}} + \frac{T_o - T_{in}}{R_{win}} + Q_{inter,in} + Q_{HVAC} \quad (2\text{-c})$$

$$C_m \frac{dT_m}{dt} = \frac{T_{in} - T_m}{R_{in,m}} + Q_{solar,m} + Q_{inter,m} \quad (2\text{-d})$$

where R and C represent the overall heat resistance and capacitance, respectively; T denotes temperature; the subscripts *in, o, w, int, ext, win,* and *m* indicate indoor air, outdoor air, exterior wall, internal wall surface, external wall surface, window, and internal mass, respectively; f denotes the conversion coefficients for the heat gains, which are also identified together with R and C; Q_{inter} denotes the internal heat gains, which consist of the heat to indoor air ($Q_{inter,in} = f_{inter,in}Q_{inter}$) and internal thermal mass ($Q_{inter,m} = f_{inter,m}Q_{inter}$); Q_{solar} denotes the heat gains from solar radiation, which include the effects on external wall surfaces ($Q_{solar,w} = f_{solar,w}A_wI_{solar}$) and internal thermal mass ($Q_{solar,m} = f_{solar,m}A_{win}I_{solar}$); I_{solar} denotes the global solar radiation; and A denotes the geometric area. The detailed model identification methods can be found in our previous publication [13].

Considering building clusters comprising thousands of households, Eqs. (2-a)–(2-d) were converted into a state-space formulation for computational efficiency, as shown in Eq. (3).

$$dT = (AT + Bu + Ed)dt \tag{3}$$

where the system state $T = [T_{w,ext} \quad T_{w,int} \quad T_{in} \quad T_m]^T$; the input vector $u = Q_{HVAC}$; the disturbance vector $d = [T_o \quad I_{solar} \quad Q_{inter}]^T$; the system matrix $A = \begin{pmatrix} \frac{-1}{C_wR_{w,o}} + \frac{-1}{C_wR_w} & \frac{1}{C_wR_w} & 0 & 0 \\ \frac{1}{C_wR_w} & \frac{-1}{C_wR_w} + \frac{-1}{C_wR_{w,in}} & \frac{1}{C_wR_{w,in}} & 0 \\ 0 & \frac{1}{C_{in}R_{w,in}} & \frac{-1}{C_{in}R_{w,in}} + \frac{-1}{C_{in}R_{in,m}} + \frac{-1}{C_{in}R_{win}} & \frac{1}{C_{in}R_{in,m}} \\ 0 & 0 & \frac{1}{C_mR_{in,m}} & \frac{-1}{C_mR_{in,m}} \end{pmatrix}_{4\times4}$; the input matrix $B = (0 \quad 0 \quad 1/C_{in} \quad 0)^T$; and the disturbance matrix $E = \begin{pmatrix} \frac{1}{C_wR_{w,o}} & \frac{f_{solar,w}\times A_w}{C_w} & 0 \\ 0 & 0 & 0 \\ \frac{1}{C_{in}R_{win}} & 0 & \frac{f_{inter,in}}{C_{in}} \\ 0 & \frac{f_{solar,m}\times A_{win}}{C_m} & \frac{f_{inter,m}}{C_m} \end{pmatrix}_{4\times3}$. Note that Eq. (3) is a continuous-time state-space model, which needs to be discretized.

3.2.2. AC performance model

AC units are widespread in residential flats in subtropical Hong Kong to ensure the thermal comfort of occupants during the hot and humid summer. Household air

conditioners are the dominant electricity consumers, representing 35% of the total electricity used in the residential sector in 2018 [6]. The cooling capacity and power of air conditioners for living/dining rooms and bedrooms are normally determined to match the peak cooling loads of the rooms. According to an earlier questionnaire-based study in Hong Kong [42], the average power ratings of air conditioners in living/dining rooms and bedrooms are 1.56 kW and 0.63 kW, respectively, which helped determine the probability distribution of the parameters of AC performance in this study.

An energy performance model of residential ACs was needed for integration with the building thermal model to predict energy consumption. The empirical model provided by DOE-2 was used in this study to predict AC performance under different operating conditions [13, 43]. The cooling capacity and energy input ratio (*EIR*) under specific operating conditions are given by Eqs. (4-a)–(4-b). A basic on/off control was used as the AC control algorithm. For this type of AC, the energy consumption during a period is mainly determined by the accumulated on-state time. Its state depends on the thermostat set-point and dead-band (δ = 1°C), as shown in Eq. (5). To protect the compressor, one state must last for at least three minutes before it is switched to another state.

$$cap = (-0.0092T_{o,db} + 1.3243)cap_{rated} \quad (4\text{-a})$$

$$EIR = (0.0193T_{o,db} + 0.3259)EIR_{rated} \quad (4\text{-b})$$

$$S = 1,\ T_i > T_{set} + \delta/2 \quad (5\text{-a})$$

$$S = 0,\ T_i \leq T_{set} - \delta/2 \quad (5\text{-b})$$

where *cap* and *EIR* denote the cooling capacity and energy input ratio (the inverse of COP) of the AC, respectively; *rated* indicates the rated operating condition [44]; and $T_{o,db}$, S, and δ denote the dry-bulb temperature of the outdoor air, operating signal, and control dead-band, respectively.

3.3. Quantification of the uncertainty in the aggregate energy flexibility of building clusters

3.3.1. Energy-flexibility control strategy

As the major electricity consumers in buildings, AC systems and equipment play significant roles in providing demand flexibility. Zone temperature set-point reset is a commonly used control strategy to reduce/shift the power consumption during on-peak

hours and to provide energy flexibility [4]. In this study, we investigated the energy flexibility of residential building clusters under the temperature set-point reset strategy.

3.3.2. Uncertainty quantification using the Monte Carlo method

Building energy consumption and energy flexibility have considerable uncertainty due to the uncertainty in outdoor weather conditions, building design/construction, HVAC system performance, occupant behavior, etc. When building clusters are scaled up, the influence of these uncertain sources on the aggregate energy flexibility is thought to change, which is not reported in the existing literature. The uncertainty qualification for various scales of building clusters can help electric utilities select a feasible service area size to provide energy-flexibility services and alleviate the power imbalance.

To combine the influence of all uncertain inputs on the system output, i.e., energy consumption/energy flexibility, the uncertainty of the input variables was first quantified based on their probability distributions. Based on the existing studies on sensitivity analysis on building design parameters [23, 24, 45], four groups of major input variables, i.e., building design, AC system design, occupancy, and occupant behavior, were selected and quantified. The quantification of uncertainty for these inputs is summarized in Table 1. A stochastic occupancy profile was then generated using the identified MCMC model. Occupancy behavior consists of two parameters: (1) the temperature set-point in the baseline case, which shows an occupant's use of their cooling system under normal conditions; and (2) the increase in temperature set-point during on-peak hours, which represents an occupant's willingness to respond to penalty signals from system operators. The commonly used Monte Carlo method [46], a sampling-based technique, was used in this study to sample over the ranges of all inputs and import the samples into the building thermal model for energy performance analysis.

Table 1. Quantification of various uncertainty sources.

Group	Parameter	Probability distribution
Building design [24]	Equivalent thermal capacitance in RC model (J/K)	U ($0.9C_{trained,}$ $1.1C_{trained}$)
	Equivalent thermal resistance in RC model (K/W)	U ($0.9R_{trained}$, $1.1R_{trained}$)
Air-conditioning system design [23]	Rated cooling capacity of AC in living room (kW)	N (3.9, 0.195^2)
	Rated cooling capacity of AC in bedroom (kW)	N (1.86, 0.093^2)
	Rated *COP* of AC in living room (kW/kW)	N (2.5, 0.125^2)
	Rated *COP* of AC in bedroom (kW/kW)	N (2.95, 0.148^2)

Occupancy	Presence states	MCMC model
Occupant behavior	Indoor air temperature set-point in the baseline case (℃)	T (23, 24, 25) *(at 0.5 ℃ intervals)*
	Temperature set-point increase during on-peak hours (℃)	T (0, 1.5, 2) *(at 0.5 ℃ intervals)*

Note: for uniform distribution U (a, b), a is the lower limit and b is the upper limit; for normal distribution N (c, d), c is the mean value and d is the variance; for triangular distribution T (e, f, g), e is the lower limit, f is the peak location, and g is the upper limit.

3.3.3. Development of performance indices for quantifying uncertainty in energy flexibility

Load shedding is a common energy-flexibility measure. To measure load shedding, the power reduction percentage is normally used as a performance index to quantify the energy flexibility [8], which was also used in this study. However, use of a performance index to quantify the uncertainty in energy flexibility has not been reported in the literature. In this subsection, two performance indices are proposed to quantify the uncertainty in energy flexibility at a specific time slot (e.g., hourly and sub-hourly) and over a particular time period (e.g., daily and weekly).

Fig. 2 illustrates the procedure for determining the uncertainty-based energy flexibility at a specific time and over a particular time period. Let the number of sampling times for uncertainty analysis be $n \in [1, 2, \dots, N]$. Then, the deterministic energy flexibility (*DEF*) at a specific time $t \in [1, 2, \dots, K]$ at the n^{th} sample can be given by Eq. (6). After *N* times of sampling, the uncertainty-based energy flexibility at a specific time *t* ($EF_t^{n=N}$) is assumed to follow the distribution of $EF_t^{n=N} \sim (\mu_{EF,t}^N, \delta_{EF,t}^N)$. Then, the uncertainty of energy flexibility (*UEF*) at a specific time *t* with *N* times of sampling ($UEF_t^{n=N}$) can be determined using the coefficient of variance (*CV*), as shown in Eq. (7), which is a standardized measure of dispersion of a probability/frequency distribution.

$$DEF_t^n = \frac{E_{baseline\ case,t}^n - E_{flexible\ case,t}^n}{E_{baseline\ case,t}^n} \tag{6}$$

$$UEF_t^{n=N} = CV_{EF,t}^N = \frac{\delta_{EF,t}^N}{\mu_{EF,t}^N} \tag{7}$$

The energy flexibility during time period Δt after *N* times of sampling ($EF_{\Delta t=[1,2,\dots,K]}^{n=N}$) can then be described by Eq. (8), and the uncertainty of energy flexibility during that time period can be described by Eq. (9).

$$EF_{\Delta t=[1,2,\dots,K]}^{n=N} \sim \left(\frac{\sum_{t=1}^K \mu_{EF,t}^N}{K}, \frac{\sum_{t=1}^K \delta_{EF,t}^N}{K}\right) \tag{8}$$

$$UEF^{n=N}_{\Delta t=[1,2,\ldots,K]} = \overline{CV}^{N}_{EF} = \frac{1}{K}\sum_{t=1}^{K}\frac{\delta^{N}_{EF,t}}{\mu^{N}_{EF,t}} \quad (9)$$

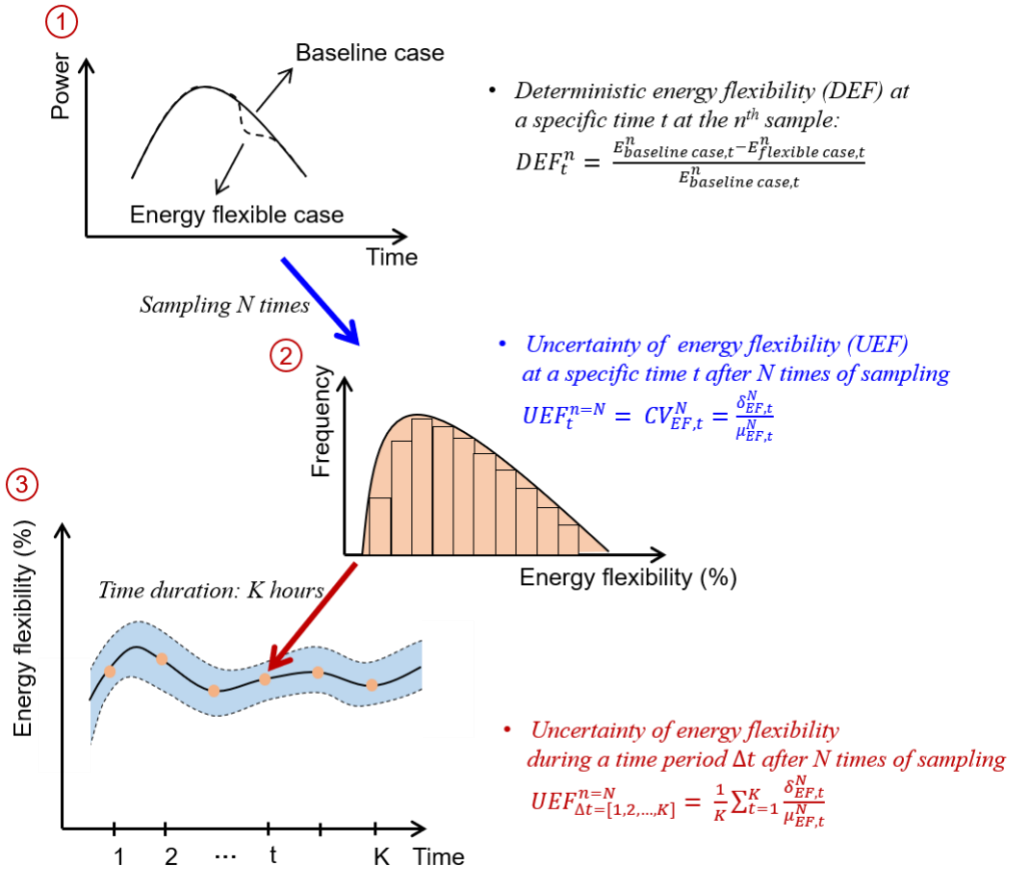

Fig. 2. Scheme of uncertainty-based energy flexibility at a specific time (e.g., hourly and sub-hourly) and over a particular time period (e.g., daily and weekly).

4. Validation and test conditions

- *Description of the reference residential building clusters*

A typical public housing estate in Hong Kong, as shown in Fig. 3-a, was chosen in this study to validate the proposed approach to quantifying the aggregate energy flexibility in residential building clusters. The target housing estate consists of 16 blocks of high-rise buildings, with standard block type of Concord-1 [47]. Each block has 40 floors and each floor consists of 8 flat units. The total number of households in the target residential community is 5120. As shown in Fig. 3-b, the flats in the east/west wings (Flats 1, 2, 5 and 6) have one living/dining room and three bedrooms, whereas the flats in the north/south wings (Flats 3, 4, 7, and 8) consist of one living/dining room and only two bedrooms. Both living/dining rooms and bedrooms are equipped with AC to provide thermal comfort during the hot and humid summer. The average household size

for a public housing household is 3.4 persons per household [39]. It is reasonable to assume that the households with 2 bedrooms and 3 bedrooms are 3-person and 4-person households, respectively. Therefore, the occupancy model for 3-person and 4-person households was used to analyze the building energy performances in the case study.

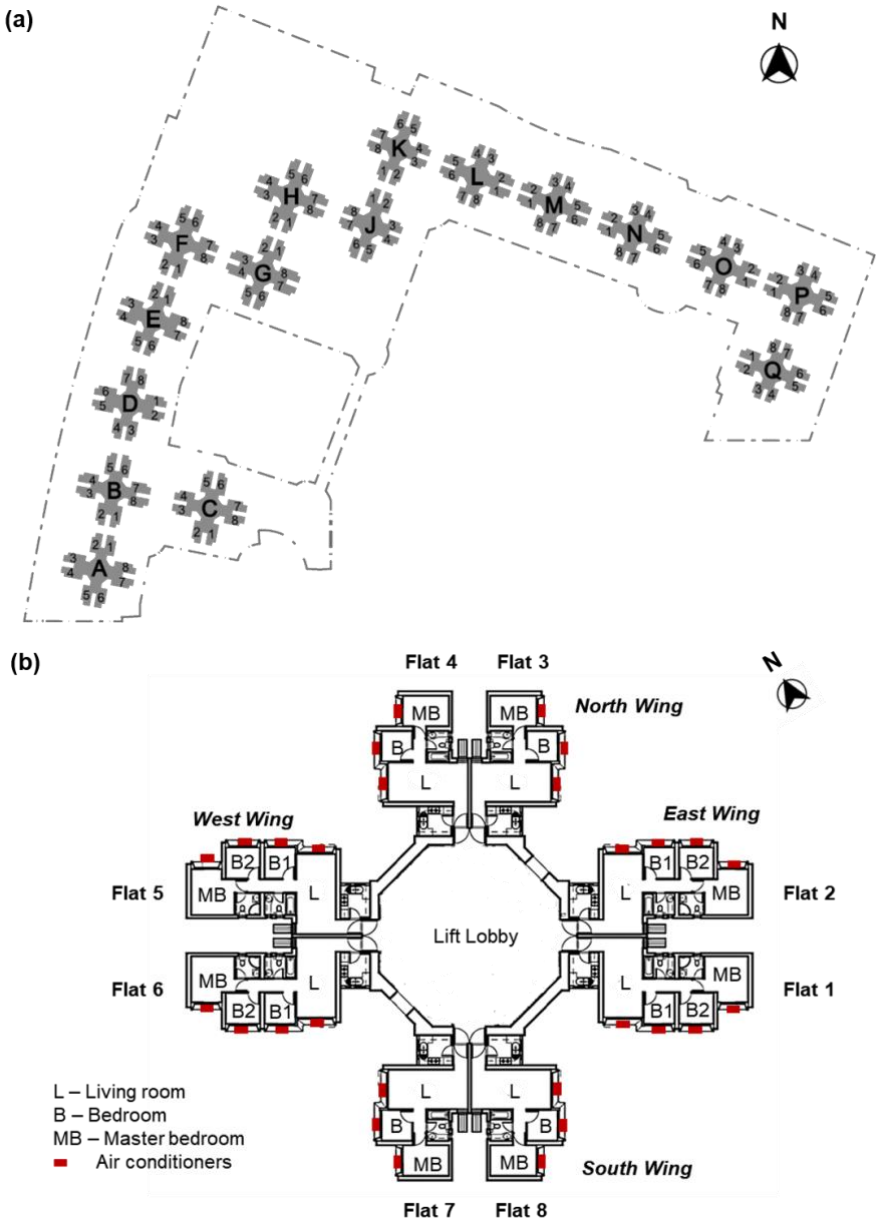

Fig. 3. a) Block layout of a typical public housing estate in Hong Kong (16 blocks; 40 floors per block); b) typical floor plan (8 flats per floor; standard block type: Concord-1).

- *Baseline case and energy-flexible case*

For comparison, the baseline AC power consumption under a conventional operating pattern, i.e., without any control strategies for energy flexibility, needed to be analyzed first. In the baseline case, the original indoor air temperature set-point of all air-

conditioned spaces was assumed to follow a triangular distribution, i.e., T (23, 24, 25) when the space is occupied. In the energy-flexible case, the increase in temperature during on-peak hours was also assumed to be subject to a triangular distribution, i.e., T (0, 1.5, 2), which shows an occupant's willingness to respond to penalty signals from system operators during on-peak hours. In the present study, building energy flexibility was assumed to be required by the system operators from 18:00 to 21:00, during which time the electricity load on the utility grid is normally at a peak in Hong Kong.

5. Results and discussion

The performances of the data-driven occupancy model and the building thermal model were analyzed first. With the identified occupancy and building thermal models, the aggregate energy performances of scaled-up residential building clusters were then investigated under both the baseline case and the energy-flexible case. Last, the uncertainty in the energy consumption and energy flexibility of scaled-up building clusters was analyzed using the Monte Carlo sampling method.

5.1. Data-driven occupancy model and building thermal model

5.1.1. Stochastic occupancy model

To analyze the effect of occupancy on uncertainty in energy flexibility, a questionnaire survey was carried out to collect occupancy time-series data to identify the data-driven Markov-chain occupancy model. A total of 155 completed and usable questionnaires were collected and used for this analysis. The collected occupancy data were categorized by (1) household size (3-person or 4 person), (2) space function (living/dining room or bedroom), and (3) day of the week (weekday or weekend/holiday). The transition probabilities at each time step for each case were identified using Eq. (1-d). Then, based on Eq. (1-c), the occupation probabilities at each time step for living rooms/bedrooms in 3-person/4-person households on weekdays/weekends were determined.

As shown in Fig. 4, the bedrooms had higher probabilities of being occupied on weekend mornings than on weekday mornings. For living rooms, the probability profiles of being occupied on weekend mornings showed certain time lags compared with those on weekday mornings, which conforms with the common practice where residents normally sleep longer on weekends and enter the living room later in the day.

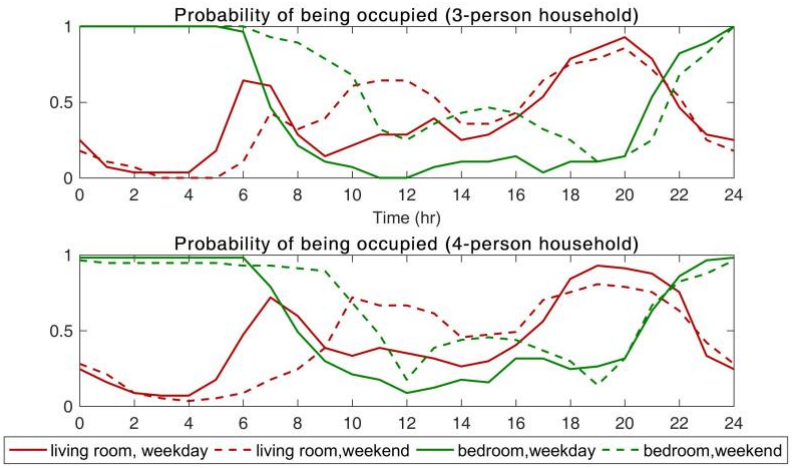

Fig. 4. Probabilities of being occupied for living room/bedroom in 3-person/4-person households on weekdays/weekends.

With the identified probabilities of occupancy states, the MCMC occupancy model was used to obtain stochastic occupancy time-series data for large-scale investigation. Fig. 5 shows the stochastic occupancy time-series data for 100 living rooms/bedrooms in a week generated by the proposed MCMC occupancy model. Living rooms have larger stochasticity in occupancy states than bedrooms because living rooms normally accommodate multiple living activities for household members. Compared with 3-person households, the occupancy states of living rooms/bedrooms in 4-person households are more uncertain due to the larger household size.

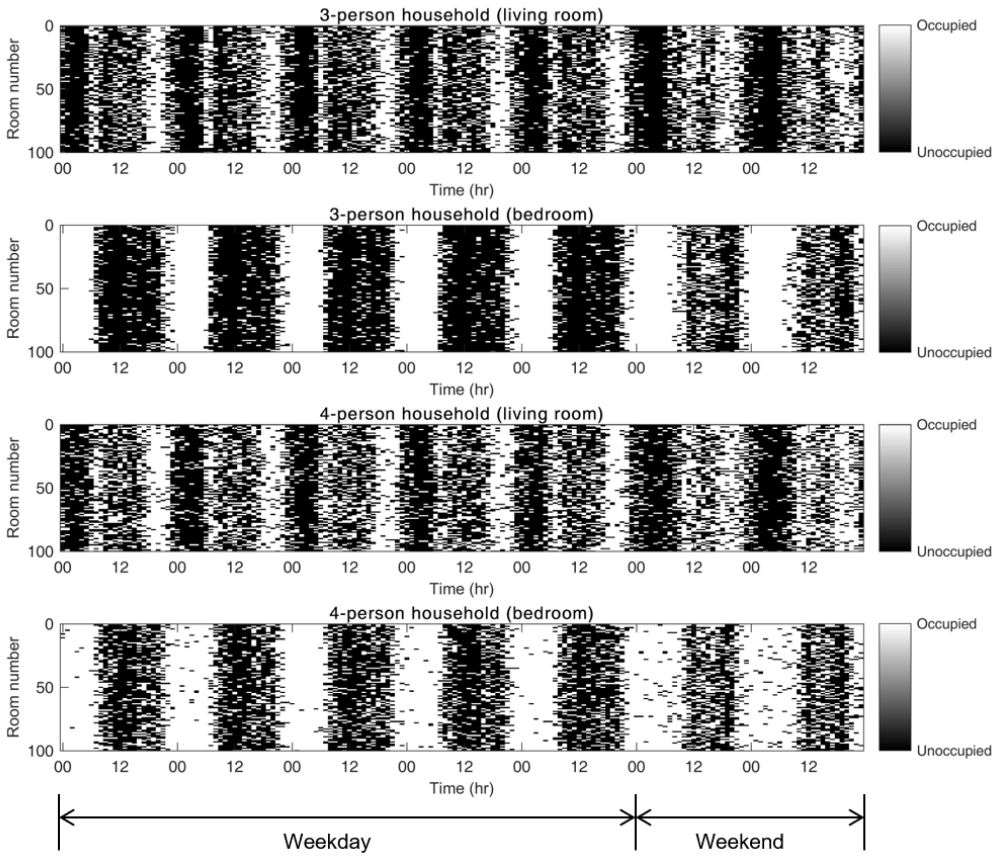

Fig. 5. Stochastic occupancy time-series data for 100 living rooms/bedrooms for a week generated by the MCMC occupancy model.

5.1.2. Building thermal model

- *Data generation for various groups of rooms*

The building thermal model (RC model) proposed in this study is a gray-box model, the parameters of which needed to be identified before applying it in forward predictions. The building thermal performance data generated from TRNSYS were used in this study to identify the RC model. To investigate differences in the thermal performance of the flats in different wings, a typical floor with eight flat units was chosen for a simulation-based case study in TRNSYS. The weather conditions consisted of outdoor air temperature and solar irradiation with various azimuth angles, as shown in Fig. 6-a. Azimuth angle-based solar irradiation was used as a model input (i.e., I_{solar} in disturbance vector d), which helped improve the model accuracy. The simulation duration was two weeks at 2-min intervals.

The thermal performances of the 16 air-conditioned rooms in the east and west wings were classified into two groups, Group 1 and Group 2, as shown in Fig. 6-b. The thermal

performances of all living rooms and non-master bedrooms in Flat 1, Flat 2, Flat 5 and Flat 6 were almost the same, and they belong to Group 1 because these rooms have north-/south-facing exterior walls and windows and solar irradiation on north-/south-facing surfaces differs little, as shown in Fig. 6-a. Group 2 includes the thermal performances of all master bedrooms in the east/west wings, which differ from those in Group 1 due to the east-/west-facing exterior walls.

Unlike the rooms in the east/west wings, the thermal performances of the 12 air-conditioned rooms in the north/south wings were classified into four groups (Groups 3–6), as shown in Fig. 6-c. The thermal performances of the living rooms and non-master bedrooms in Flat 3/Flat 8 (Group 3) differed from those in Flat 4/Flat 7 (Group 4) due to large variations in solar irradiation on the east-/west-facing surfaces, as shown in Fig. 6-a. Group 5 and Group 6 represent the thermal performances of the master bedrooms in Flat 3/Flat 8 and Flat 4/Flat 7, respectively, which differed from those in Group 3 and Group 4 due to the north-/south-facing exterior walls.

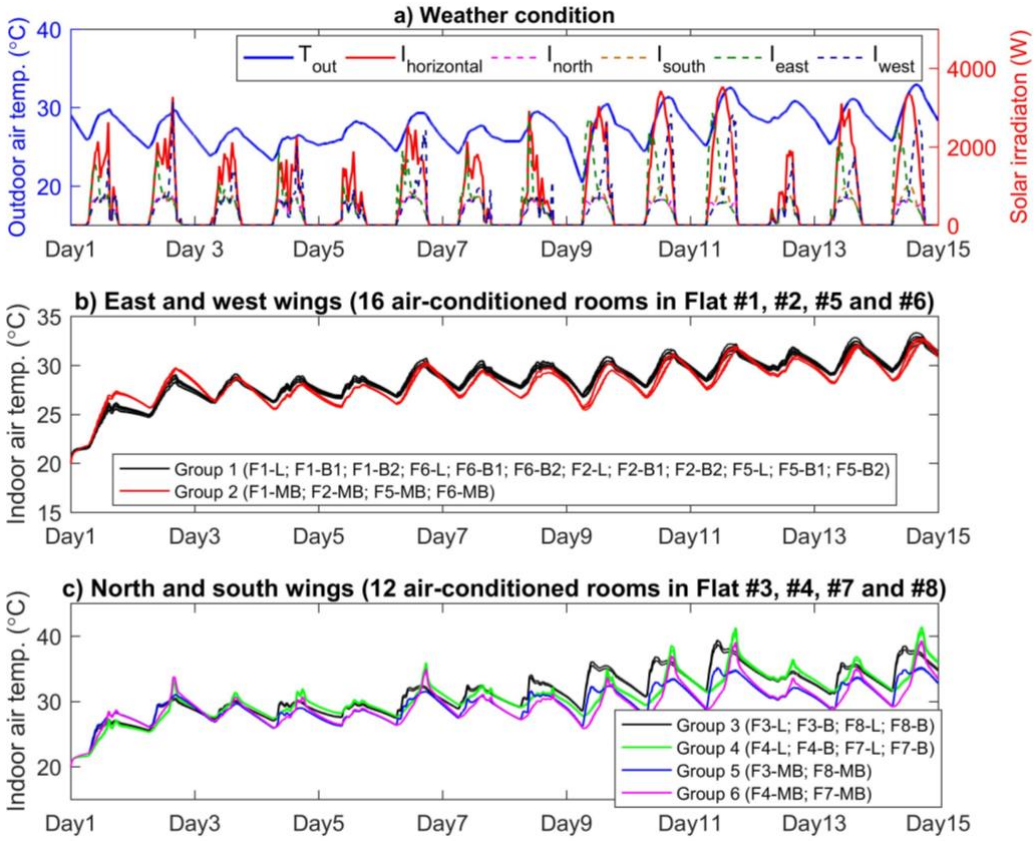

Fig. 6. (a) Weather condition, (b) thermal performances of the flats in the east and west wings, and (c) thermal performances of the flats in the north and south wings.

- *Model identification for various groups of rooms*

Each group of indoor air temperature profiles at 2-min intervals generated from TRNSYS was used to identify the building thermal model. The identified R and C values in the RC model for each group of buildings are listed in Table 2. The root-mean-square errors (RMSEs) between the performance data from TRNSYS and those from the RC model for two weeks were 0.305°C, 0.403°C, 0.479°C, 0.450°C, 0.493°C, and 0.462°C for Groups 1–6, respectively. As shown in Fig. 7, the results show that the RC room thermal model can predict the indoor air temperature with a relatively high degree of accuracy.

Table 2. Identified R and C values in RC models for various groups of rooms.

	Group 1	**Group 2**	**Group 3**	**Group 4**	**Group 5**	**Group 6**
C_w (J/K)	218,817	735,823	218,817	218,817	364,089	364,089
C_{in} (J/K)	306,776	295,118	205,164	236,933	194,032	181,696
C_m (J/K)	7,001,954	3,727,102	7,536,269	6,829,379	3,677,106	3,098,612
R_{win} (K/W)	0.0220	0.0220	0.0220	0.0220	0.0220	0.0220
R_w (K/W)	0.0406	0.0406	0.0406	0.0406	0.0406	0.0406
$R_{w,o}$ (K/W)	0.0035	0.0038	0.0059	0.0051	0.0026	0.0032
$R_{w,in}$ (K/W)	0.0085	0.0085	0.0085	0.0085	0.0085	0.0085
$R_{in,m}$ (K/W)	0.0054	0.0062	0.0067	0.0065	0.0069	0.0076
$f_{solar,w}$	1.0000	1.0000	1.0000	1.0000	1.0000	1.0000
$f_{solar,m}$	0.1100	0.0000	0.1343	0.1357	0.0650	0.0418
$f_{inter,in}$	2.0000	2.0000	2.5927	2.6804	2.0015	2.2479
$f_{inter,m}$	2.0000	2.0000	1.7746	1.6621	2.4762	2.3630
RMSE (°C)	**0.305**	**0.403**	**0.479**	**0.450**	**0.493**	**0.461**

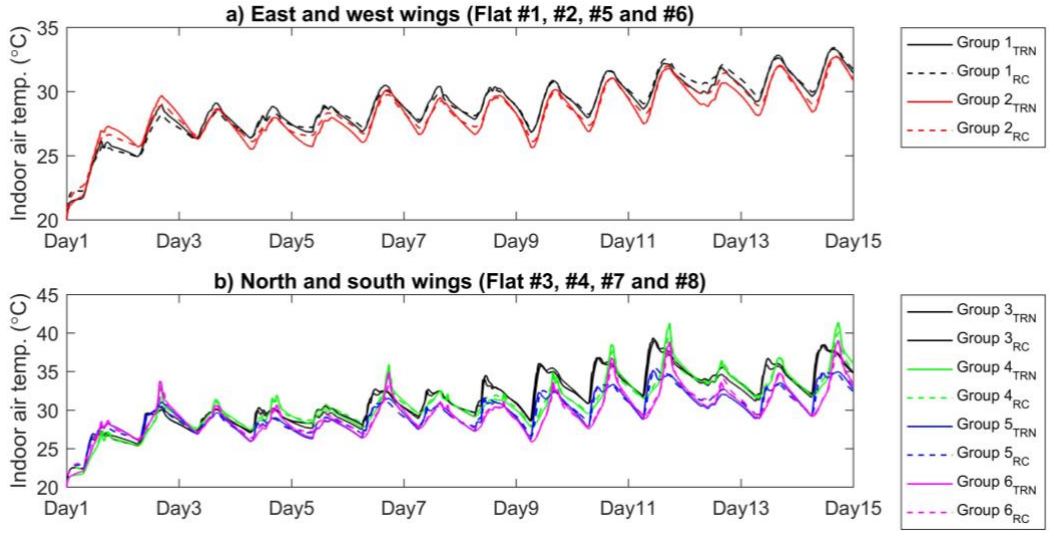

Fig. 7. Comparison between the thermal performances by TRNSYS and the RC model for various groups of rooms in (a) east/west wings and (b) north/south wings.

5.2. Deterministic energy flexibility of building clusters of various scales

With the developed data-driven stochastic occupancy model and building thermal model, the deterministic aggregate energy performances of scaled-up building clusters were analyzed under both the baseline case and energy-flexible case. The energy performance is called deterministic because the sampling and simulation were conducted only once. The case studies were carried out for one week, and the weather conditions from Day 8 to Day 14 in Fig. 6-a were used to test the energy performance of the building clusters. For comparative study, the scales of the building clusters were increased from 8 households (1 floor) to 80 households (10 floors), 320 households (40 floors, 1 block), 640 households (80 floors, 2 blocks), 1280 households (160 floors, 4 blocks), 2560 households (320 floors, 8 blocks) and 5,120 households (640 floors, 16 blocks). Note that for better illustration, the simulation results with the sizes of 640, 1280 and 2560 households are not plotted in some figures.

5.2.1. Deterministic energy consumption in baseline case

Fig. 8 shows the thermal and energy performances of individual living rooms/bedrooms and the aggregate energy performances for scaled-up building clusters in the baseline case. As shown in Fig. 8-a (8 households), different patterns of the indoor air temperature were found due to different designs of building envelope parameters and building orientations, which validates that the developed model is sensitive to different building designs and weather conditions. When the living rooms/bedrooms were occupied, the indoor air temperature was maintained around the set-point, which was subject to the triangular distribution of T (23, 24, 25), to provide indoor thermal comfort. The power consumption of individual ACs around noon was higher than that during other time periods because the higher outdoor temperature at noon resulted in higher AC energy consumption, which validates that the AC model used in this study is sensitive to outdoor air conditions. Compared with bedrooms, living rooms had more stochasticity in their thermal and energy performances because the occupancy states of living rooms were more stochastic. Regarding the aggregated power profile, ACs in living rooms accounted for the majority of electricity use in the daytime, whereas ACs in bedrooms represented the majority of electricity use at nighttime. Also, ACs in both living rooms and bedrooms consumed more electricity on weekends than on weekdays because residents generally stayed home more on weekends.

For comparison analysis, the thermal and energy performances of individual rooms and the aggregate energy performance of the baseline case scaled up to 80, 320, and 5,120 households were tested, and the results are shown in Fig. 8-b, Fig. 8-c, and Fig. 8-d, respectively. The aggregate power consumption increased when the building cluster was scaled up. Moreover, the aggregate power consumption of the larger scales of building clusters showed less fluctuation/volatility compared with that of small scales of building clusters.

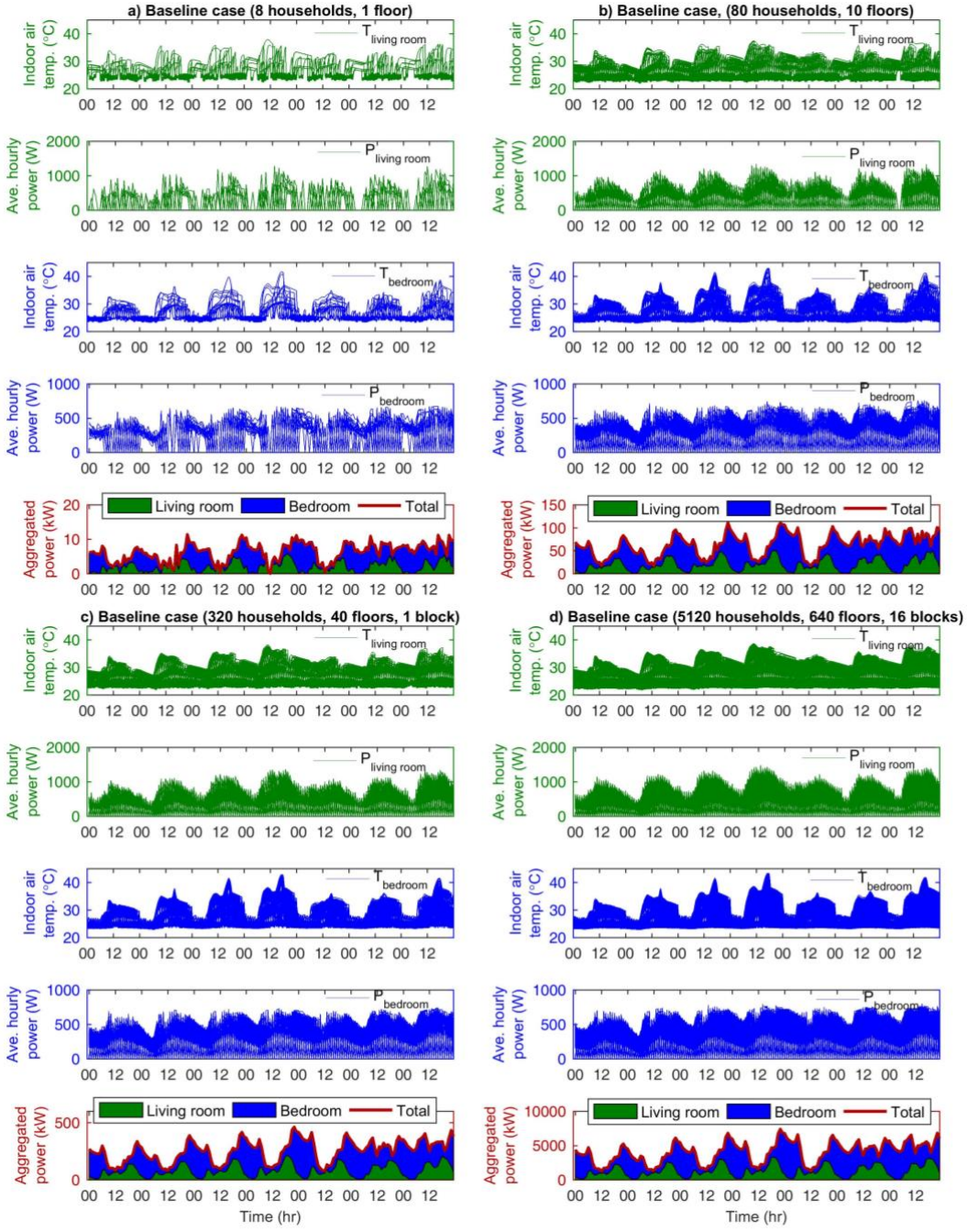

Fig. 8. ***Deterministic baseline case***: thermal (indoor air temperature) and energy performances of individual living rooms/bedrooms and aggregate energy consumption for building clusters of various scales for one week: (a) 8 households, (b) 80 households, (c) 320 households, and (d) 5,120 households.

5.2.2. Deterministic aggregate energy flexibility

Fig. 9 shows the thermal and energy performances of individual living rooms/bedrooms and the aggregate energy performance for scaled-up building clusters in the energy-flexible case. The temperature set-points in the living rooms/bedrooms were increased during on-peak hours (18:00–21:00) in the energy-flexible case. The increase in temperature set-point followed a triangular distribution, i.e., T (0, 1.5, 2). As shown in Fig. 9-a, the indoor air temperature in the living rooms/bedrooms increased somewhat during energy-flexible hours, resulting in power reductions. Like the baseline case, the aggregate power consumption profiles of the larger scales of building clusters fluctuated less, as shown in Figs. 9-b–9-d.

After obtaining the energy performance profiles of the baseline and energy-flexible cases, the deterministic energy flexibility of various scales of building clusters were quantified using Eq. (6). As shown in Fig. 10, the daily deterministic energy flexibility in a week was 9.81%–16.7% for 8 households, 10.07%–15.69% for 80 households, 10.04%–16.11% for 320 households, and 9.99%–16.01% for 5,120 households. A power spike occurred right after implementation of energy-flexible control strategies, while aggregating the power consumption of the building clusters. This power spike is often called “power rebound”, which has adverse effects on the power grid and needs to be addressed in future work.

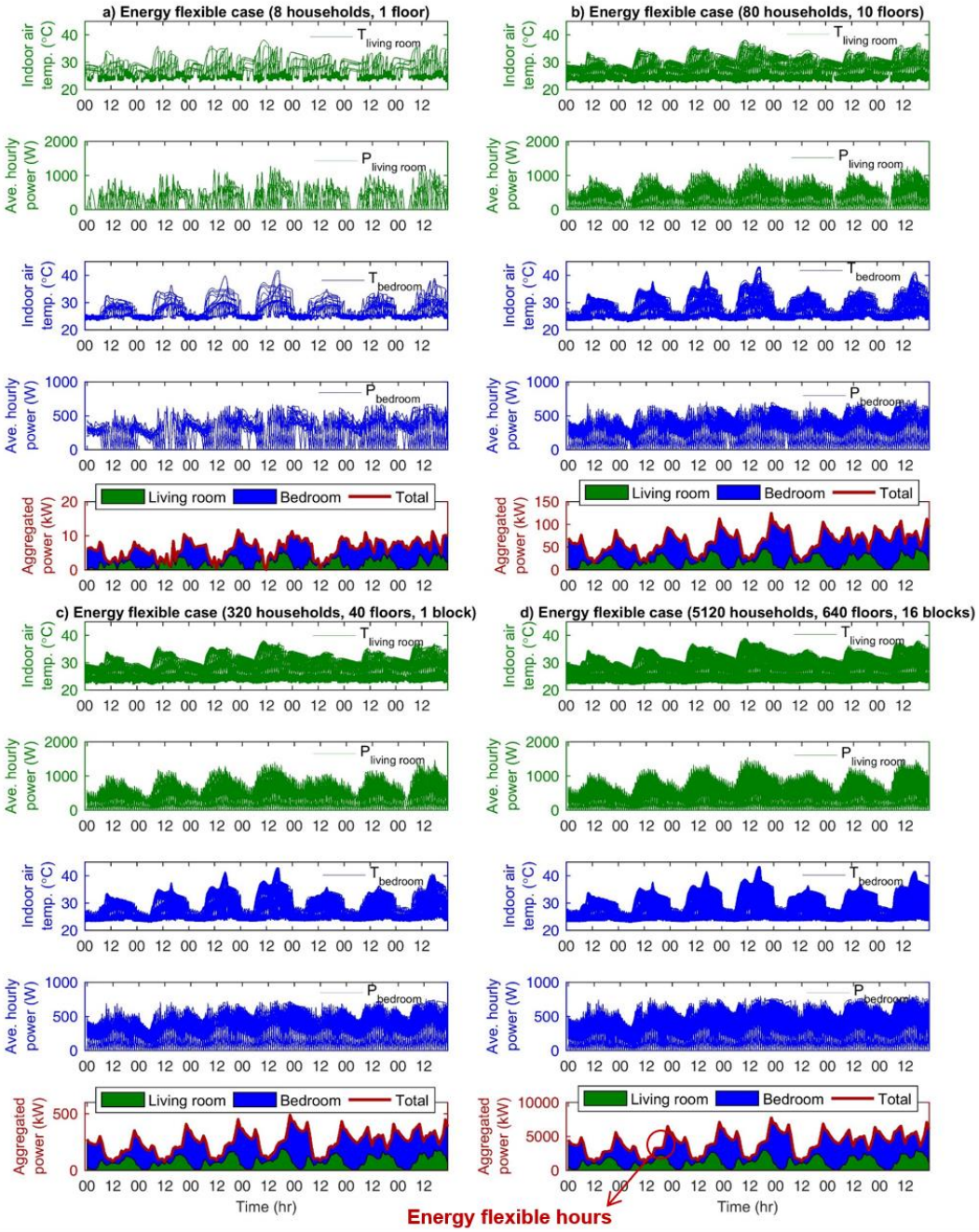

Fig. 9. ***Deterministic energy-flexible case***: thermal (indoor air temperature) and energy performances of individual living rooms/bedrooms and aggregate energy consumption for building clusters of various scales for one week: (a) 8 households, (b) 80 households, (c) 320 households, and (d) 5,120 households.

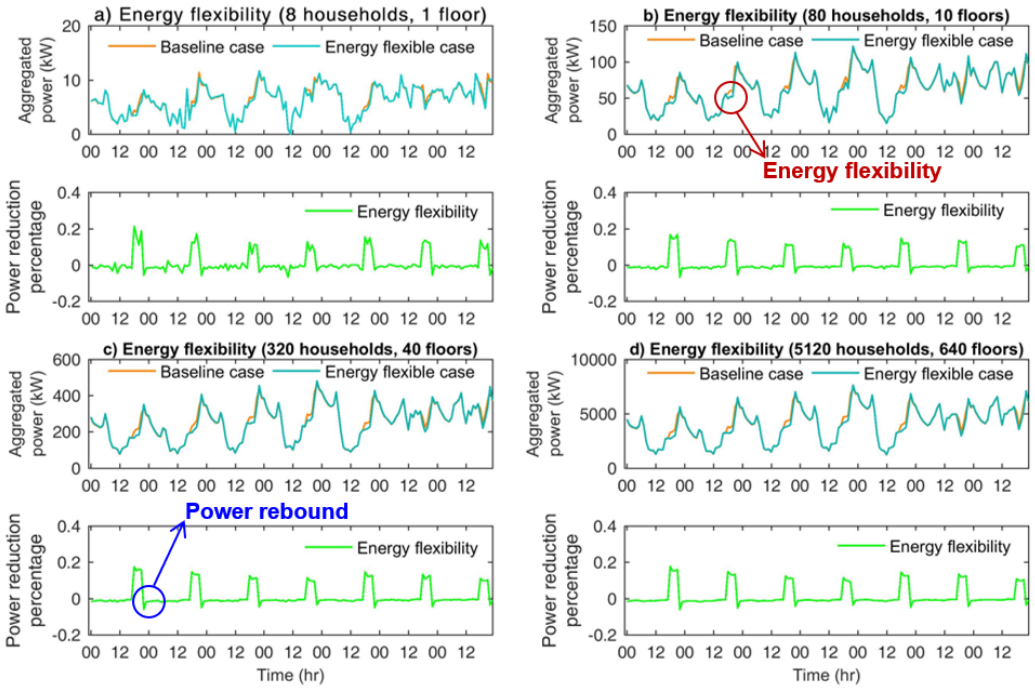

Fig. 10. ***Deterministic energy flexibility***: quantification of the aggregate energy flexibility for building clusters of various scales for one week: (a) 8 households, (b) 80 households, (c) 320 households, and (d) 5,120 households.

5.3. Uncertainty-based energy flexibility of building clusters of various scales

To quantify the uncertainty in aggregate energy consumption and energy flexibility, the energy performance of various scales of building clusters were simulated 1,000 times. Each time, the building envelope parameters, AC rated performance, occupancy, and occupancy behavior were sampled using the Monte Carlo method.

5.3.1. Uncertainty in aggregate energy consumption

Fig. 11 shows the uncertainty in the aggregate energy consumption of scaled-up building clusters in the baseline and energy-flexible cases. The width of the uncertainty "band" decreases as the building cluster is scaled up. For specific comparison, the uncertainty of energy consumption each hour was quantified using the index of *CV* and the results are plotted in Fig. 12. The uncertainty of energy consumption for 8 households is much larger than that for the scaled-up households. The hourly uncertainty during the day normally reached a peak around noon due to the high transition probability of occupancy, as shown in Fig. 5, and the high power consumption of AC at noon. The energy consumption on weekends has a flatter profile of uncertainty compared with that on weekdays.

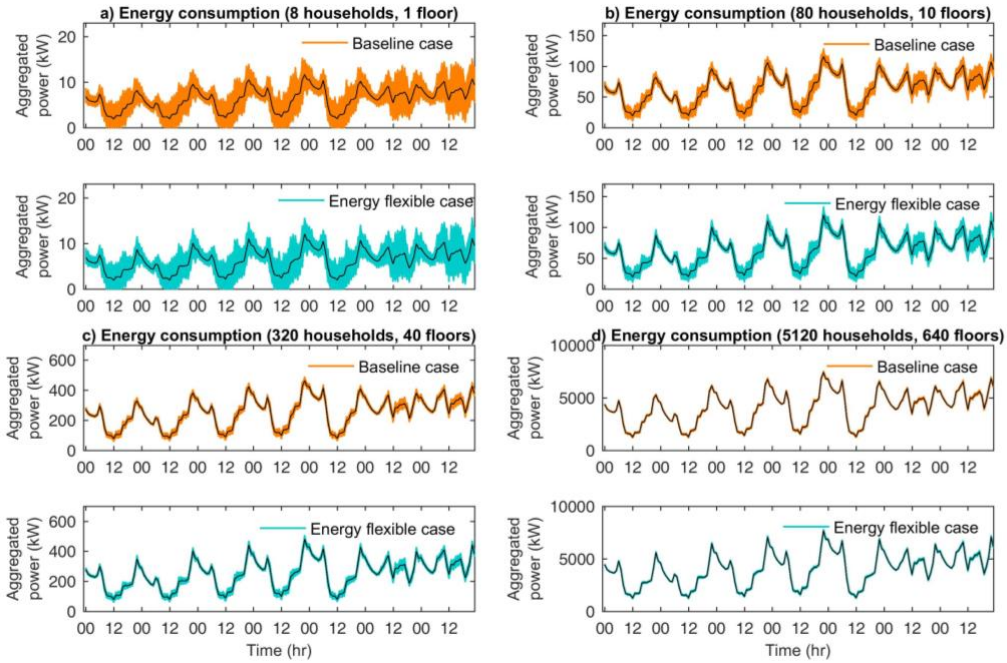

Fig. 11. ***Uncertainty-based energy consumption***: hourly uncertainty-based energy consumption in the baseline and energy-flexible cases for building clusters of various scales: (a) 8 households, (b) 80 households, (c) 320 households, and (d) 5,120 households.

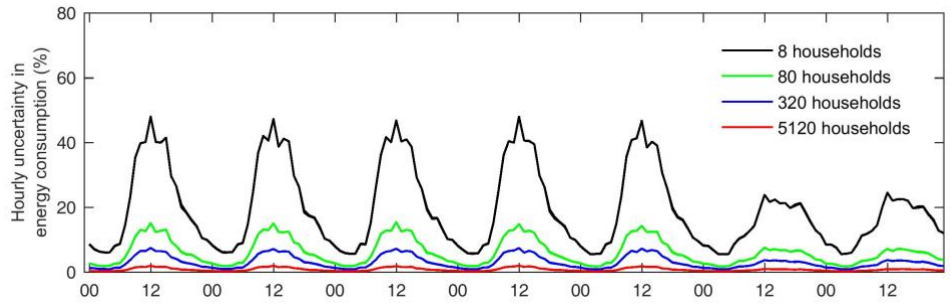

Fig. 12. Hourly uncertainty of aggregate energy consumption for building clusters of various scales.

5.3.2. Uncertainty in aggregate energy flexibility

The hourly energy flexibility was derived based on the hourly energy consumption in the baseline and energy-flexible cases. Only the energy flexibility and its uncertainty during energy-flexible hours (18:00–21:00) were taken into consideration. Fig. 13 shows the hourly uncertainty-based energy flexibility for building clusters of various scales. Table 3 shows the maximum and minimum hourly uncertainty of energy flexibility (*UEF*) of scaled-up building clusters. As we can see from Fig. 13 and Table 3, at the same scale of household, the hourly *UEF* differed over the time because it was affected by the weather conditions, occupancy and occupant behavior. When the buildings cluster was scaled up, the hourly uncertainty of aggregated energy flexibility

had a significant decrease on the same day. For example, on Day 7, the maximum hourly uncertainty of energy flexibility, $UEF_{hourly,max}$, decreased from 25.01% for 8 households to 1.00% for 5120 households.

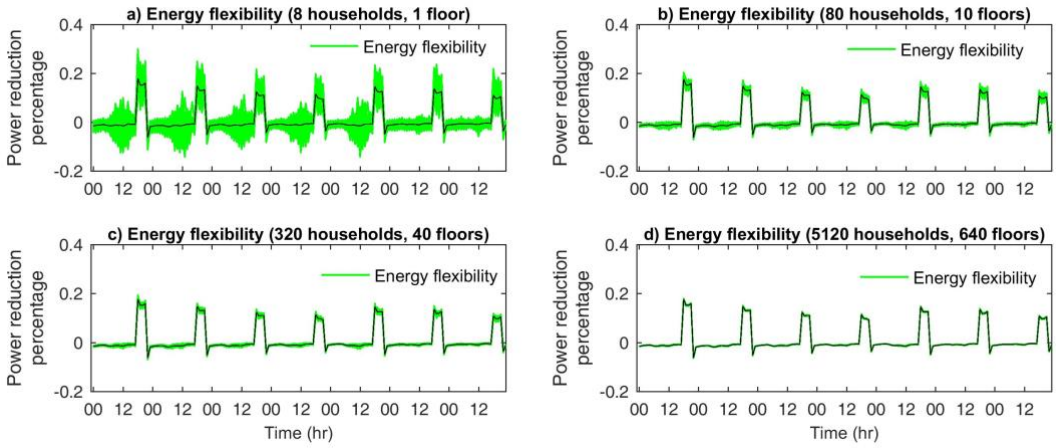

Fig. 13. ***Uncertainty-based energy flexibility***: hourly uncertainty-based energy flexibility for building clusters of various scales: (a) 8 households, (b) 80 households, (c) 320 households, and (d) 5,120 households.

Table 3. Hourly uncertainty of aggregate energy flexibility of scaled-up building clusters

		Number of Households						
		8	80	320	640	1280	2560	5120
Day 1	$UEF_{hourly,min}$	14.12%	4.46%	2.27%	1.55%	1.10%	0.79%	0.53%
	$UEF_{hourly,max}$	19.38%	6.07%	3.06%	2.18%	1.52%	1.12%	0.73%
Day 2	$UEF_{hourly,min}$	15.04%	4.86%	2.33%	1.66%	1.20%	0.82%	0.59%
	$UEF_{hourly,max}$	20.60%	6.17%	3.17%	2.17%	1.57%	1.11%	0.80%
Day 3	$UEF_{hourly,min}$	17.86%	5.20%	2.65%	1.84%	1.33%	0.95%	0.67%
	$UEF_{hourly,max}$	21.73%	6.68%	3.49%	2.35%	1.69%	1.17%	0.82%
Day 4	$UEF_{hourly,min}$	18.95%	5.91%	3.04%	2.18%	1.51%	1.03%	0.76%
	$UEF_{hourly,max}$	22.99%	6.97%	3.57%	2.54%	1.81%	1.27%	0.90%
Day 5	$UEF_{hourly,min}$	15.34%	4.74%	2.49%	1.70%	1.23%	0.88%	0.61%
	$UEF_{hourly,max}$	20.26%	6.28%	3.24%	2.24%	1.60%	1.15%	0.82%
Day 6	$UEF_{hourly,min}$	16.20%	5.18%	2.47%	1.81%	1.29%	0.91%	0.63%
	$UEF_{hourly,max}$	23.79%	7.13%	3.57%	2.44%	1.77%	1.24%	0.84%
Day 7	$UEF_{hourly,min}$	18.31%	5.56%	2.80%	1.94%	1.42%	1.00%	0.71%
	$UEF_{hourly,max}$	25.01%	7.94%	4.01%	2.67%	1.94%	1.36%	1.00%

Based on the hourly performance, the daily aggregate energy flexibility and its uncertainty were calculated using the proposed performance index, i.e., Eqs. (8) and (9). The detailed results are listed in Table 4 and plotted in Fig. 14. As shown in Table 4, the daily energy flexibility ($\bar{\mu}_{EF,daily}$) in one week were 10.06%–16.05% for 8 households, 10.01%–15.95% for 80 households, 10.01%–15.98% for 320 households, and 10.01%–15.97% for 640, 1280, 2560 and 5,120 households. The weekly energy

flexibility ($\bar{\mu}_{EF,weekly}$) was 12.39% for 8 households and 12.35% for scaled-up households. Regarding the uncertainty of energy flexibility , the daily uncertainty of energy flexibility (UEF_{daily}) in one week was 17.08%–21.33% for 8 households, 5.37%–6.63% for 80 households, 2.67%–3.28% for 320 households, 1.87%-2.38% for 640 households, 1.33%-1.65% for 1280 households, 0.96%-1.17% for 2560 households and 0.64%–0.83% for 5,120 households. As shown in Fig. 14, the daily uncertainty of aggregate energy flexibility exponentially decreased with the scaling up of building clusters. The weekly uncertainty of energy flexibility (UEF_{weekly}) was 19.12% for 8 households, 5.91% for 80 households, 2.95% for 320 households, 2.08% for 640 households, 1.48% for 1280 households, 1.05% for 2560 households, and 0.74% for 5,120 households.

In conclusion, when the building clusters were scaled up, the daily/weekly energy flexibility exhibited little change. The daily energy flexibility was 10%–16% and the weekly energy flexibility remained around 12.40%. Unlike the energy flexibility, the uncertainty of energy flexibility (UEF) exhibited a significant decrease when the number of aggregate buildings increased. The weekly uncertainty of energy flexibility (UEF_{weekly}) exponentially decreased from 19.12% for 8 households to 0.74% for 5,120 households.

Table 4. Daily and weekly uncertainty of aggregate energy flexibility of scaled-up building clusters.

		Number of Households						
		8	80	320	640	1280	2560	5120
Day 1	$\bar{\mu}_{EF,daily}$	16.05%	15.95%	15.98%	15.97%	15.97%	15.97%	15.97%
	$\bar{\sigma}_{EF,daily}$	2.74%	0.86%	0.43%	0.30%	0.21%	0.15%	0.10%
	UEF_{daily}	**17.08%**	**5.37%**	**2.67%**	**1.87%**	**1.33%**	**0.96%**	**0.64%**
Day 2	$\bar{\mu}_{EF,daily}$	13.49%	13.49%	13.49%	13.50%	13.50%	13.50%	13.50%
	$\bar{\sigma}_{EF,daily}$	2.49%	0.76%	0.38%	0.26%	0.19%	0.13%	0.10%
	UEF_{daily}	**18.47%**	**5.66%**	**2.79%**	**1.95%**	**1.41%**	**0.99%**	**0.70%**
Day 3	$\bar{\mu}_{EF,daily}$	11.31%	11.31%	11.31%	11.31%	11.31%	11.31%	11.31%
	$\bar{\sigma}_{EF,daily}$	2.26%	0.69%	0.35%	0.24%	0.17%	0.12%	0.09%
	UEF_{daily}	**20.00%**	**6.08%**	**3.07%**	**2.16%**	**1.52%**	**1.09%**	**0.76%**
Day 4	$\bar{\mu}_{EF,daily}$	10.06%	10.01%	10.01%	10.01%	10.01%	10.01%	10.01%
	$\bar{\sigma}_{EF,daily}$	2.13%	0.64%	0.33%	0.24%	0.17%	0.12%	0.08%
	UEF_{daily}	**21.17%**	**6.40%**	**3.28%**	**2.38%**	**1.65%**	**1.15%**	**0.82%**
Day 5	$\bar{\mu}_{EF,daily}$	13.03%	13.05%	13.04%	13.04%	13.04%	13.04%	13.04%
	$\bar{\sigma}_{EF,daily}$	2.40%	0.74%	0.37%	0.26%	0.19%	0.13%	0.10%
	UEF_{daily}	**18.40%**	**5.68%**	**2.87%**	**2.01%**	**1.43%**	**1.02%**	**0.73%**
Day 6	$\bar{\mu}_{EF,daily}$	12.53%	12.45%	12.46%	12.46%	12.46%	12.46%	12.46%
	$\bar{\sigma}_{EF,daily}$	2.37%	0.74%	0.36%	0.26%	0.18%	0.13%	0.09%

Day 7	UEF_{daily}	**18.96%**	**5.96%**	**2.92%**	**2.07%**	**1.47%**	**1.04%**	**0.74%**
	$\bar{\mu}_{EF,daily}$	10.23%	10.16%	10.18%	10.17%	10.17%	10.17%	10.17%
	$\bar{\sigma}_{EF,daily}$	2.18%	0.67%	0.33%	0.23%	0.17%	0.12%	0.08%
	UEF_{daily}	**21.33%**	**6.63%**	**3.28%**	**2.31%**	**1.65%**	**1.17%**	**0.83%**
Average	$\bar{\mu}_{EF,weekly}$	12.39%	12.35%	12.35%	12.35%	12.35%	12.35%	12.35%
	$\bar{\sigma}_{EF,weekly}$	2.37%	0.73%	0.36%	0.26%	0.18%	0.13%	0.09%
	UEF_{weekly}	**19.12%**	**5.91%**	**2.95%**	**2.08%**	**1.48%**	**1.05%**	**0.74%**

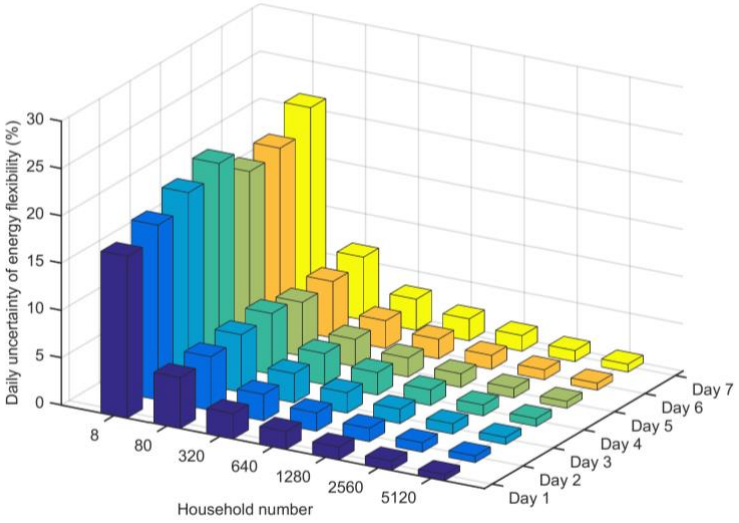

Fig. 14. Daily uncertainty of aggregate energy flexibility for various scales of building clusters.

6. Conclusions

In this study, we developed an approach for quantifying the uncertainty in the aggregate energy flexibility of residential buildings at a cluster/community/neighborhood level. The aggregation and uncertainty analyses were conducted based on the development of a data-driven stochastic occupancy model and a data-driven building thermal dynamics model. The major conclusions of this study are as follows:

- A data-driven stochastic occupancy model was developed based on the Markov-chain Monte Carlo method. Because Hong Kong has its own special domestic housing types, household sizes, and household composition types, a customized questionnaire survey was carried out to collect occupancy time-series data to determine the occupancy model. The developed occupancy model captured the dynamics, stochasticity, and diversity in occupancy patterns considering the effects of household size (3-person or 4 person), space function (living/dining room or bedroom), and day of the week (weekday or weekend/holiday) in Hong Kong. This model can be integrated into building energy performance simulation tools such as EnergyPlus and HK-BEAM to consider the uncertainty in occupancy.

- Aggregation analysis was conducted to quantify the aggregate energy flexibility of residential building clusters considering various types of building archetypes and occupancy patterns. For each air-conditioned room, the developed stochastic occupancy model was integrated with the data-driven building thermal model developed to predict building energy performance under a baseline case and an energy-flexible case, resulting in the energy-flexibility potential.
- Performance indices were proposed to quantify the uncertainty in energy flexibility at a specific time (e.g., hourly and sub-hourly) and the uncertainty during a particular time period (e.g., daily and weekly). Based on the proposed performance indices, the uncertainty in the aggregate energy flexibility of various scales of building clusters was quantified using the Monte Carlo sampling technique. The results showed that when the building cluster were scaled up, the energy flexibility remained almost unchanged and the weekly energy flexibility remained around 12.40%. However, when the number of aggregate buildings increased, the uncertainty of energy flexibility significantly decreased. The weekly uncertainty exponentially decreased from 19.12% for 8 households to 0.74% for 5,120 households.

Due to the intrinsic uncertainty in building envelope parameters, the performance of building energy systems, and occupancy and occupant behavior, it is necessary to quantify the uncertainty in the aggregate energy flexibility of building clusters. The proposed method can help energy providers/load aggregators consider the uncertainty in the aggregate energy flexibility potential. The uncertainty analysis results can assist them with the planning of energy-flexibility services at the design stage and the development of real-time penalty signals (e.g., prices and CO_2) at the operating stage. In the future, an advanced control strategy needs to be further developed to address the ‘‘power rebound’’ issue, which was found by aggregation analysis in this study.

Acknowledgments

The research work presented in this paper was financially supported by a research grant (G-YBTB) from the Hong Kong Polytechnic University (PolyU) and the Strategic Focus Area (SFA) Scheme (1-BBW7) of the Research Institute for Sustainable Urban Development (RISUD) in PolyU. The support is gratefully acknowledged. The authors would also like to acknowledge Chin Man Leung, an undergraduate student in PolyU, for helping with the questionnaire survey.

References

[1] Niknam T, Golestaneh F, Malekpour A. Probabilistic energy and operation management of a microgrid containing wind/photovoltaic/fuel cell generation and energy storage devices based on point estimate method and self-adaptive gravitational search algorithm. Energy. 2012;43:427-37.

[2] Neves D, Brito MC, Silva CA. Impact of solar and wind forecast uncertainties on demand response of isolated microgrids. Renewable Energy. 2016;87:1003-15.

[3] Wang S, Xue X, Yan C. Building power demand response methods toward smart grid. HVAC&R Research. 2014;20:665-87.

[4] Chen Y, Xu P, Gu J, Schmidt F, Li W. Measures to improve energy demand flexibility in buildings for demand response (DR): A review. Energy and Buildings. 2018;177:125-39.

[5] Somasundaram S, Pratt R, Akyol B, Fernandez N, Foster N, Katipamula S, et al. Reference guide for a transaction-based building controls framework. Pacific Northwest National Laboratory. 2014.

[6] EMSD. Hong Kong Energy End-use Data 2018. Electrical and Mechanical Services Department. 2018.

[7] Wang S. Making buildings smarter, grid-friendly, and responsive to smart grids. Science and Technology for the Built Environment. 2016;22:629-32.

[8] Jensen SØ, Marszal-Pomianowska A, Lollini R, Pasut W, Knotzer A, Engelmann P, et al. IEA EBC Annex 67 Energy Flexible Buildings. Energy and Buildings. 2017;155:25-34.

[9] Le Dréau J, Heiselberg P. Energy flexibility of residential buildings using short term heat storage in the thermal mass. Energy. 2016;111:991-1002.

[10] Shafie-khah M, Kheradmand M, Javadi S, Azenha M, de Aguiar JLB, Castro-Gomes J, et al. Optimal behavior of responsive residential demand considering hybrid phase change materials. Applied Energy. 2016;163:81-92.

[11] Finck C, Li R, Kramer R, Zeiler W. Quantifying demand flexibility of power-to-heat and thermal energy storage in the control of building heating systems. Applied Energy. 2018;209:409-25.

[12] Yin R, Kara EC, Li Y, DeForest N, Wang K, Yong T, et al. Quantifying flexibility of commercial and residential loads for demand response using setpoint changes. Applied Energy. 2016;177:149-64.

[13] Hu M, Xiao F, Wang L. Investigation of demand response potentials of residential air conditioners in smart grids using grey-box room thermal model. Applied Energy. 2017;207:324-35.

[14] Hu M, Xiao F. Price-responsive model-based optimal demand response control of inverter air conditioners using genetic algorithm. Applied Energy. 2018;219:151-64.

[15] Turner WJN, Walker IS, Roux J. Peak load reductions: Electric load shifting with mechanical pre-cooling of residential buildings with low thermal mass. Energy. 2015;82:1057-67.

[16] Hu M, Xiao F, Jørgensen JB, Li R. Price-responsive model predictive control of floor heating systems for demand response using building thermal mass. Applied Thermal Engineering. 2019;153:316-29.

[17] Vigna I, Pernetti R, Pasut W, Lollini R. New domain for promoting energy efficiency: Energy Flexible Building Cluster. Sustainable Cities and Society. 2018;38:526-33.

[18] Taniguchi A, Inoue T, Otsuki M, Yamaguchi Y, Shimoda Y, Takami A, et al. Estimation of the contribution of the residential sector to summer peak demand reduction in Japan using an energy end-use simulation model. Energy and Buildings. 2016;112:80-92.

[19] Perfumo C, Kofman E, Braslavsky JH, Ward JK. Load management: Model-based control of aggregate power for populations of thermostatically controlled loads. Energy Conversion and Management. 2012;55:36-48.

[20] Goy S, Finn D. Estimating Demand Response Potential in Building Clusters. Energy Procedia. 2015;78:3391-6.

[21] Wang A, Li R, You S. Development of a data driven approach to explore the energy flexibility potential of building clusters. Applied Energy. 2018;232:89-100.

[22] Tian W, Heo Y, de Wilde P, Li Z, Yan D, Park CS, et al. A review of uncertainty analysis in building energy assessment. Renewable and Sustainable Energy Reviews. 2018;93:285-301.

[23] Huang P, Huang G, Sun Y. Uncertainty-based life-cycle analysis of near-zero energy buildings for performance improvements. Applied Energy. 2018;213:486-98.

[24] Domínguez-Muñoz F, Cejudo-López JM, Carrillo-Andrés A. Uncertainty in peak cooling load calculations. Energy and Buildings. 2010;42:1010-8.

[25] Huang P, Huang G, Wang Y. HVAC system design under peak load prediction uncertainty using multiple-criterion decision making technique. Energy and Buildings. 2015;91:26-36.

[26] de Wilde P, Tian W, Augenbroe G. Longitudinal prediction of the operational energy use of buildings. Building and Environment. 2011;46:1670-80.

[27] Eguaras-Martínez M, Vidaurre-Arbizu M, Martín-Gómez C. Simulation and evaluation of Building Information Modeling in a real pilot site. Applied Energy. 2014;114:475-84.

[28] Yan D, Hong T, Dong B, Mahdavi A, D'Oca S, Gaetani I, et al. IEA EBC Annex 66: Definition and simulation of occupant behavior in buildings. Energy and Buildings. 2017;156:258-70.

[29] Happle G, Fonseca JA, Schlueter A. A review on occupant behavior in urban building energy models. Energy and Buildings. 2018;174:276-92.

[30] Naylor S, Gillott M, Lau T. A review of occupant-centric building control strategies to reduce building energy use. Renewable and Sustainable Energy Reviews. 2018;96:1-10.

[31] Richardson I, Thomson M, Infield D. A high-resolution domestic building occupancy model for energy demand simulations. Energy and Buildings. 2008;40:1560-6.

[32] Wilke U, Haldi F, Scartezzini J-L, Robinson D. A bottom-up stochastic model to predict building occupants' time-dependent activities. Building and Environment. 2013;60:254-64.

[33] Yan D, O'Brien W, Hong T, Feng X, Burak Gunay H, Tahmasebi F, et al. Occupant behavior modeling for building performance simulation: Current state and future challenges. Energy and Buildings. 2015;107:264-78.

[34] Zhang Y, Bai X, Mills FP, Pezzey JCV. Rethinking the role of occupant behavior in building energy performance: A review. Energy and Buildings. 2018;172:279-94.

[35] Page J, Robinson D, Morel N, Scartezzini JL. A generalised stochastic model for the simulation of occupant presence. Energy and Buildings. 2008;40:83-98.

[36] Widén J, Nilsson AM, Wäckelgård E. A combined Markov-chain and bottom-up approach to modelling of domestic lighting demand. Energy and Buildings. 2009;41:1001-12.

[37] McKenna E, Krawczynski M, Thomson M. Four-state domestic building occupancy model for energy demand simulations. Energy and Buildings. 2015;96:30-9.

[38] Census and Statistics Department. Hong Kong Annual Digest of Statistics. Hong Kong: Census and Statistics Department; 2018.

[39] Census and Statistics Department. 2016 Population By-census – Summary Results. Hong Kong: Census and Statistics Department; 2016.

[40] Serale G, Fiorentini M, Capozzoli A, Bernardini D, Bemporad A. Model Predictive Control (MPC) for Enhancing Building and HVAC System Energy Efficiency: Problem Formulation, Applications and Opportunities. Energies. 2018;11:631.

[41] Cigler J, Gyalistras D, Široky J, Tiet V, Ferkl L. Beyond theory: the challenge of implementing model predictive control in buildings. Proceedings of 11th Rehva world congress, Clima2013.

[42] Chen H, Lee WL. Combined space cooling and water heating system for Hong Kong residences. Energy and Buildings. 2010;42:243-50.

[43] York DA, Tucker EF. DOE-2 Reference Manual Part 1 Version 2.1. Los Alamos, New Mexico: Los Alamos Scientific Laboratory; 1980.

[44] ANSI/AHRI. Standard for Performance Rating of Unitary Air-Conditioning and Air-Source Heat Pump Equipment. Arlington, VA: Air-Conditioning, Heating, and Refrigeration Institute; 2008.

[45] Li H, Wang S, Cheung H. Sensitivity analysis of design parameters and optimal design for zero/low energy buildings in subtropical regions. Applied Energy. 2018;228:1280-91.

[46] Hammersley J. Monte carlo methods: Springer Science & Business Media; 2013.

[47] Hong Kong Housing Authority. Standard Block Typical Floor Plans. 2019. Available: https://www.housingauthority.gov.hk/en/global-elements/estate-locator/standard-block-typical-floor-plans/index.html